Available online at www.sciencedirect.com
ScienceDirect
Journal of Non-Crystalline Solids 354 (2008) 263–268
JOURNAL OF NON-CRYSTALLINE SOLIDS
www.elsevier.com/locate/jnoncrysol

Specific heat of ethanol at low temperatures

Virginia Rodriguez-Mora, Miguel A. Ramos *

LBT-UAM, Departamento de Física de la Materia Condensada, C-III, Universidad Autónoma de Madrid, Cantoblanco, 28049 Madrid, Spain

Available online 24 October 2007

Abstract

We present here new specific heat measurements at low temperatures (2–20 K) of the different phases of ethanol, characterized by the same calorimetric set-up at higher temperatures. We have extended and improved earlier measurements by implementing higher-accuracy calorimetric methods at low temperatures (using two complementary versions of the thermal relaxation method), as well as at higher temperatures (using a quasi-adiabatic, continuous method). The quantitatively very similar low temperature properties and glass-transition features of both structural glass and orientationally-disordered crystal of ethanol provide clear evidence that the lack of long-range crystalline order typical of amorphous solids is an unimportant factor regarding the universal properties of glasses. We have also employed these new measuring methods to study the possible effect of water impurities on the specific heat of the different solid phases of ethanol, and to study possible variations in the specific heat between different found phases of the monoclinic crystal of ethanol.

PACS: 65.60.+a; 65.40.Ba; 61.43.Fs

Keywords: Glass-transition; Calorimetry; Thermodynamics; Water in glass

1. Introduction

It is well known [1,2] that glasses or amorphous solids exhibit universal thermal properties at low temperatures, which are in turn very different from those of crystalline solids. Its origin remains, however, one of the major unsolved and debated problems of condensed matter physics [3], together with the phenomenon of the glass-transition itself. Below 1 K, the specific heat C_p of glasses is much larger and the thermal conductivity κ orders of magnitude lower than the corresponding values found in their crystalline counterparts. C_p depends approximately linearly ($C_p \propto T$) and κ almost quadratically ($\kappa \propto T^2$) on temperature. This is in clear contrast to the cubic dependences observed in crystals for both properties, well understood in terms of Debye's theory of lattice vibrations. Above 1 K, C_p still deviates strongly from the expected $C_{\mathrm{Debye}} \propto T^3$ dependence, exhibiting a broad maximum in C_p/T^3 which is directly related to the so-called *boson peak* observed by neutron or Raman vibrational spectroscopies. In the same temperature range the thermal conductivity exhibits an ubiquitous *plateau*. These and other 'anomalous' low temperature properties of amorphous solids [2] (at least for $T < 1$ K) were soon well accounted by the tunneling model (TM) [2,4,5], whose fundamental postulate was the general existence of small groups of atoms in amorphous solids which can tunnel between two configurations of very similar energy (two-level systems, TLS). However, also the rich universal behavior of glasses above 1 K (the broad maximum in C_p/T^3, the corresponding boson peak in vibrational spectra, or the above-mentioned plateau in the thermal conductivity) was still unexplained. Among the different approaches proposed since then to understand the general behavior of glasses in the whole range of low-frequency excitations, the phenomenological soft-potential model (SPM), which can be regarded as an extension of the TM, is one of the best accepted and most often considered. The SPM (see reviews in Refs. [6,7]) postulates the coexistence in glasses of acoustic phonons (crystalline-like, extended lattice vibrations) with quasilocalized low-frequency (*soft*) modes.

* Corresponding author. Tel.: +34 91 4975551; fax: +34 91 4973961.
E-mail address: miguel.ramos@uam.es (M.A. Ramos).

0022-3093/$ - see front matter © 2007 Elsevier B.V. All rights reserved.
doi:10.1016/j.jnoncrysol.2007.07.039

Ethanol (CH_3CH_2OH) is a very well known chemical substance, widely used in daily life. However, from the scientific point of view, pure ethanol also exhibits a very interesting polymorphism [8–11] presenting different solid phases below its melting point at 159 K: the conventional, amorphous glass, obtained by quenching the supercooled liquid below the glass-transition temperature $T_g = 98 \pm 1$ K; a (bcc) plastic crystal which by quenching below the same $T_g = 98 \pm 1$ K becomes an orientationally-disordered crystal (ODC) with glassy properties (sometimes named '*glassy crystal*' [8]); and fully-ordered (monoclinic) crystals. Ethanol thus appears as a good model system to investigate abovementioned low temperature properties of glasses [1,2], including the role played by orientational vs translational disorder. Indeed, we have shown [9–11] that both the structural (amorphous) glass and the orientational glass (i.e., a crystal with orientational disorder) phases of ethanol show, qualitatively and even quantitatively, the same glassy features in the low temperature specific heat (i.e., TLS and boson peak, the latter also observed by inelastic neutron scattering [9]), altogether with very similar glass-transition phenomena between their corresponding ergodic and non-ergodic states.

Now, we have continued that previous work [9–11] by implementing higher-accuracy calorimetric methods for low temperatures (both quasi-adiabatic and thermal relaxation ones) and also for higher temperatures in the transformation range (by using a quasi-adiabatic continuous method), which can be run in the same experimental set-up. We compare our results with previous published data, and also have studied the effect of water impurities on the calorimetric and thermodynamic behavior of the different solid phases of ethanol.

2. Experimental techniques and materials

Low temperature specific heat measurements and calorimetric characterizations of the solid phases of ethanol prepared above ~100 K, were conducted in the same kind of copper calorimetric cells previously described [10,11]. A silicon diode was used as thermometer in the higher temperature range and a commercially-calibrated carbon resistor was used at lower temperatures. A 1 kΩ resistor was employed as electrical heater. The temperature of the internal vacuum chamber was controlled automatically. Small copper cells were employed (typically with 3.3 g of addenda and 2 cm^3 of liquid volume, with a thin copper mesh fitted inside to facilitate thermal equilibrium). The heat capacity of one empty cell was measured independently and under the very same conditions in order to subtract its contribution, both at low and at higher temperatures. Small differences in weight (<5%) among different cells were taken in account by considering the specific heat of copper. Experiments were run in a glass cryostat, using either nitrogen or helium as cryogenic liquids, and were conducted in a high-vacuum environment ($\leqslant 10^{-7}$ mbar). In the present work, we have employed 'dry' ethanol (Merck, nominal maximum H_2O content: 0.02%), pro-analysis ethanol (Merck, nominal maximum H_2O content: 0.1%), and commercial ethanol (Panreac, 96% v/v pure) to study the possible influence of water content on the thermodynamic and kinetic properties of ethanol. We did not make any further purification and the real amount of water impurity in ethanol samples was confirmed by measuring the index of refraction at 20 °C and comparing it with literature [12]. For our 96% v/v pure commercial ethanol, we determined a water content of $3.4 \pm 0.7\%$. Errors in water content are estimations based on the interpolation scheme using literature data, that is the main error source in this case.

Nevertheless, in contrast to the adiabatic method previously used [9–11], we have now employed a thermal relaxation method [13,14], by connecting the sample holder to the temperature-controlled thermal reservoir through a copper wire as thermal link, chosen as to have relaxation time $\tau \sim 10^2$ s in the relevant temperature range.

As a matter of fact, we have implemented an automatized calorimetric program, that allows to choose among quasi-adiabatic, continuous and thermal relaxation methods [14] to measure heat capacity C_p at low temperatures, controlling the temperature T_0 of the thermal bath in a double-chamber cryogenic insert. In the thermal relaxation method (see Fig. 1(a)), the temperature T of the sample is raised by around 1% and then let to decay exponentially with time t

$$T(t) = T_0(t) + \Delta T_\infty \exp(-t/\tau), \tag{1}$$

where ΔT_∞ is the long-time, steady-state temperature increase in the sample produced by the applied heating power P. The heat capacity is $C_p = K \cdot \tau$, with $K = P/\Delta T_\infty$. When the relaxation time τ is getting longer, we can replace the long-time heating step by a shorter heating curve (see curve (b) in Fig. 1) following:

$$T(t) = T_0(t) + \Delta T_\infty [1 - \exp(-t/\tau)]. \tag{2}$$

In this alternative relaxation method, ΔT_∞ is not measured directly, but determined from a simple linear fit of the heating curve (2), after having determined τ from the relaxation curve (1). As seen in the inset of Fig. 1, the excellent linear behavior of the semilogarithmic plot guarantees the existence of a well defined relaxation time τ for the thermal link and improves the accuracy of the measurement.

For measurements above 77 K, specific heat was measured by means of a quasi-adiabatic, continuous method. The calorimetric cell is in contact with the thermal reservoir at 77 K through an effective thermal link (mainly arising from blackbody thermal radiation plus conduction through the electrical wiring). Therefore, the equation of heat transport contains both a cooling P_{cool} and a heating P_{heat} power terms, so that

$$C_p\left(\frac{dT}{dt}\right) = P_{heat} + P_{cool} = V_h I_h + C_p \Theta(T), \tag{3}$$

where V_h and I_h are the voltage applied to the heater element, and the electric current flowing through it,

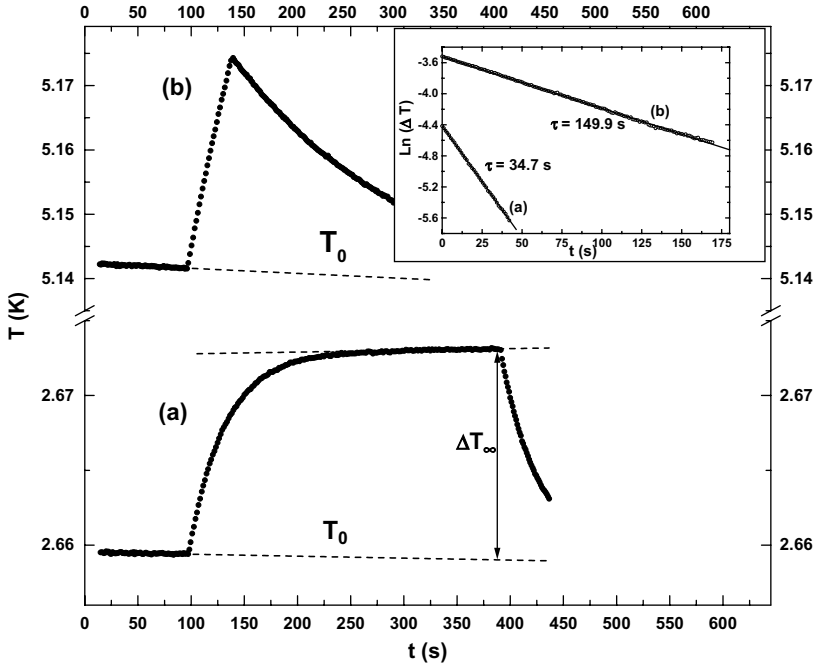

Fig. 1. Examples of real experimental points obtained for glassy ethanol using the standard relaxation method (a) and the alternative relaxation method (b), explained in the text. Inset: semilogarithmic plot used to determine via Eq. (1) the time constant τ for these experimental points.

respectively, and $\Theta(T) \equiv (\mathrm{d}T/\mathrm{d}t)_{\mathrm{drift}}$ is the intrinsic (negative) thermal drift of the system, which is directly measured as a function of temperature by standard cooling at $I_h = 0$, with the thermal reservoir fixed at 77 K. Therefore, the heat capacity of the cell can be determined from

$$C_p = \frac{V_h I_h}{\left(\frac{\mathrm{d}T}{\mathrm{d}t} - \Theta(T)\right)}. \tag{4}$$

Furthermore, a direct display of the measured $\mathrm{d}T/\mathrm{d}t$ curve as a function of temperature T, for a constant applied power, is also a useful method to monitor first-order transitions such as melting and crystallization processes. Fig. 2 depicts the main representative cases: cooling and heating curves are displayed for both pure (left panels) and commercial (right panels) ethanol. Stable γ-crystal [15] is obtained by slowly cooling the liquid of pure ethanol well below its melting temperature $T_m = 159$ K, which is observed in its heating curve at a given constant power. When the liquid is cooled at a faster rate (typically between -1 and -15 K/min), the γ crystallization is bypassed, and the supercooled liquid (SCL) enters the plastic crystal (PC) phase at $T_{pl} \approx 125$ K, and eventually the orientationally-disordered (*glassy*) crystalline phase (ODC) below 98 K. When heated, the PC phase exhibits a first-order transition into a more stable, monoclinic α-crystal, similar to, though slightly different from the γ-crystal [15]. The glass phase was not obtained in these experiments, since the needed quenching rate (faster than -20 K/min) was not achieved in the employed experimental set-up. On the other hand, commercial ethanol with around 3.4% of water does not exhibit the ODC/PC phases and the true (amorphous) glass is readily obtained with very slow cooling rates. The crystal state was obtained by heating the glass up to around 137 K. The melting temperature of this commercial ethanol is observed to occur at $T_m = 151 \pm 1$ K, eight degrees below that of pure ethanol (see Ref. [16] for more details). Errors given for transition temperatures include those from the thermal sensor and from the methods used in its determination.

3. Results and discussion

When cooling and heating curves such as those in Fig. 2 are analyzed through Eq. (4), the specific heat can be determined. Fig. 3 shows the obtained results for the glass–SCL transition in commercial (96% pure) ethanol and for the *glassy* dynamic ODC → PC transition in 99.9% pure ethanol. The big overshoots observed at the glass-transition temperatures (either the standard glass → SCL one, or the dynamic ODC → PC transition) are due to the slowly cooling rates used for their preparation, compared to the typically used heating rates around +1.5 K/min. Using the midpoint of the discontinuity in C_p to determine the glass-transition temperature [16], we obtain $T_g = 102 \pm 1$ K for commercial ethanol (glass) and $T_g = 98 \pm 1$ K for pure ethanol (ODC). Specific heat of the corresponding stable, monoclinic crystals are also shown. No difference among the different varieties of monoclinic crystals is found within experimental error. A very good agreement with earlier data from Haida et al. [8] is found in all cases for pure ethanol [16].

In Fig. 4, we present some raw heat capacity data at low temperatures for the different phases of pure (pro-analysis,

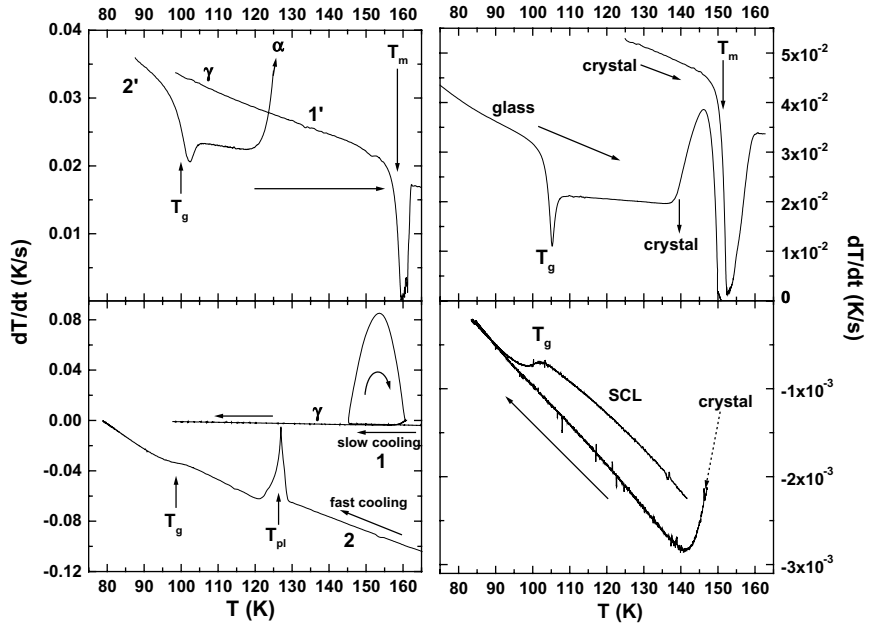

Fig. 2. Left panels: calorimetric cooling (below) and heating (above) curves using pure (pro-analysis, <0.1% H_2O) ethanol. Routes 1/1′ correspond to the cooling/heating curves for stable γ-crystal and routes 2/2′ correspond to ODC–PC phases. Right panels: calorimetric cooling (lower) and heating (upper) curves using commercial (96% v/v pure, 3.4% H_2O) ethanol.

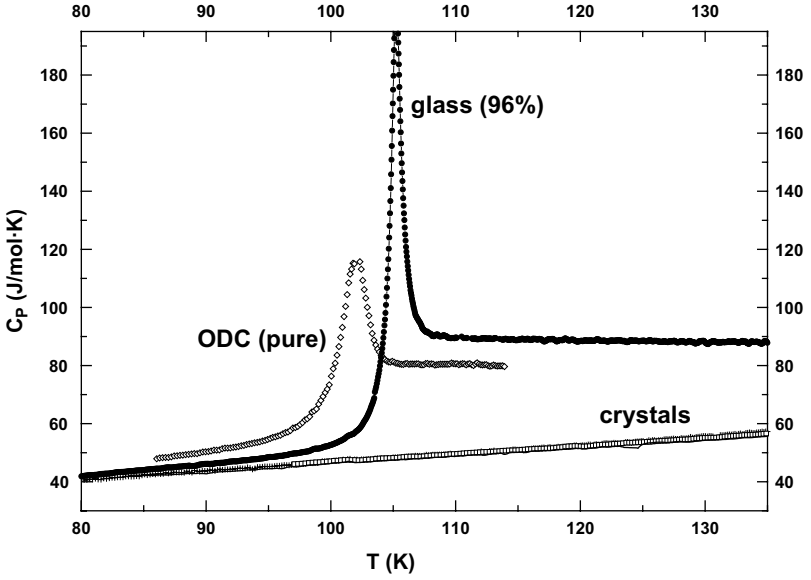

Fig. 3. Molar specific heat for the standard glass-transition in commercial (96% pure) ethanol (●) and for the *glassy* dynamic ODC → PC transition in 99.9% pure ethanol (◇). Specific heat of the corresponding stable, monoclinic crystals are shown indistinguishably: α-crystal (+) and γ-crystal (□) for pure ethanol, and only crystal (solid line) for commercial ethanol.

0.1% water) ethanol, together with the measurement of the empty cell. After subtracting the latter and dividing by the corresponding amount of ethanol in each case, molar specific heat is obtained and presented in Figs. 5 and 6 for pure and commercial ethanol, respectively. In both cases, a C_p/T^3 vs T plot is presented, which emphasizes the broad ('boson') peak at low temperatures characteristic of glassy behavior, in contrast with the horizontal Debye level of fully-ordered crystals. As previously discussed [9–11], it is noteworthy the very similar boson peak observed in the amorphous glass and in the ODC phase, which exhibits the same glassy behavior in all respects, even quantitatively. On the other hand, a slight but measurable difference in C_p has been found between γ and α crystalline phases, as can be seen in Figs. 4 and 5. This is in contrast with the behavior at higher temperatures (Fig. 3) where they were found to be identical within experimental error.

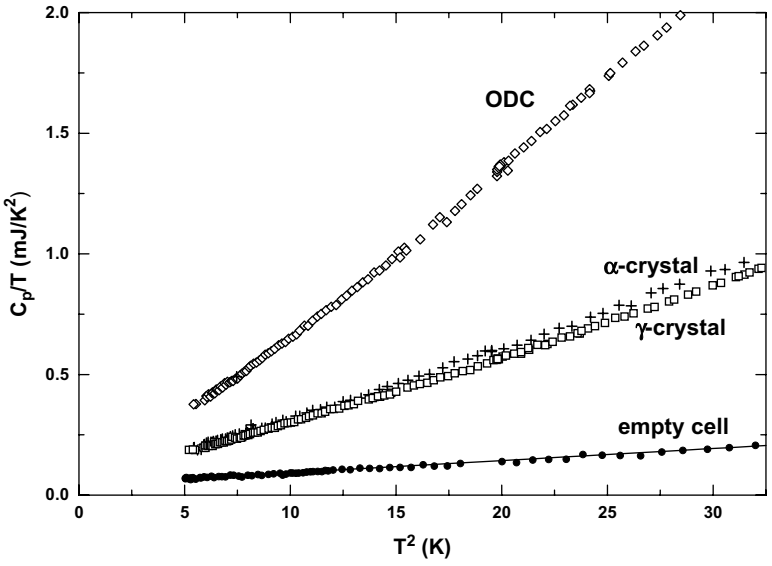

Fig. 4. Low temperature heat capacity in a C_p/T vs T^2 plot, measured with pure (0.1%) ethanol, in ODC (◇),α-crystal (+) and γ-crystal (□) phases, as well as the heat capacity measured for the empty cell (●).

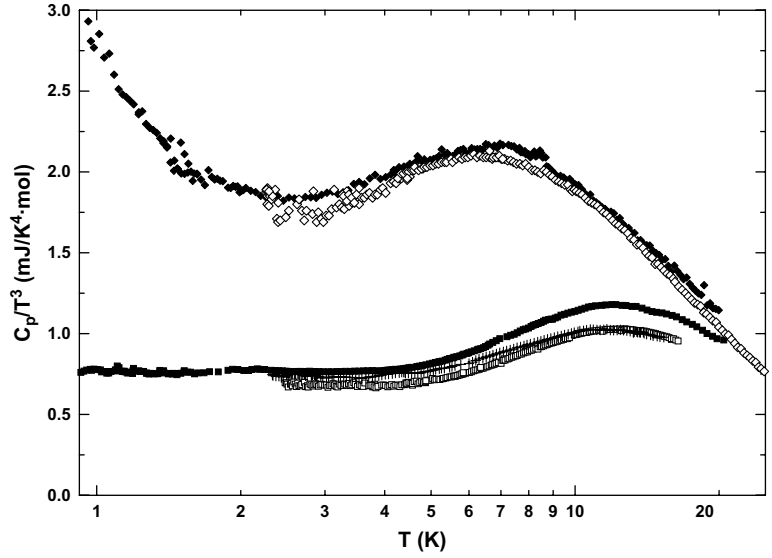

Fig. 5. Specific heat at low temperatures in a logarithmic C_p/T^3 vs T plot for ODC (◇), α-crystal (+) and γ-crystal (□) phases of pure ethanol. Solid symbols (ODC, diamonds above; crystal, squares below) are our previously published data [10,11] employing the adiabatic method in a ^{3}He-cryostat.

We also want to point out that all shown low temperature $C_p(T)$ curves contain experimental points from the two alternative relaxation methods described above. The good agreement found between both methods is a further proof of consistency to assure the higher-accuracy of these measurements, in absolute terms, compared to our previous ones. This can be seen in Fig. 5, where our previously published data [10,11] of the same phases for pure ethanol are also shown. In Fig. 6, the more appreciable differences between our earlier data for the glass and crystal phases and the recent ones are obviously due to the different purity of the samples. Water impurity (3.4%) present in commercial ethanol appears to decrease the specific heat, especially for the glass phase. On the other hand, no difference has been found between using 'dry' or 'pro-analysis' ethanol, neither in specific heat values nor in glassy or crystalline kinetics. In all the cases studied by us up to now, either employing dry or pro-analysis ethanol, the amount of water measured after the calorimetric experiments was always below $0.19 \pm 0.25\%$, slightly different amounts of measured impurity being likely due to different history and care taken to avoid air moisture when manipulating the samples, rather to the initial purity of the product.

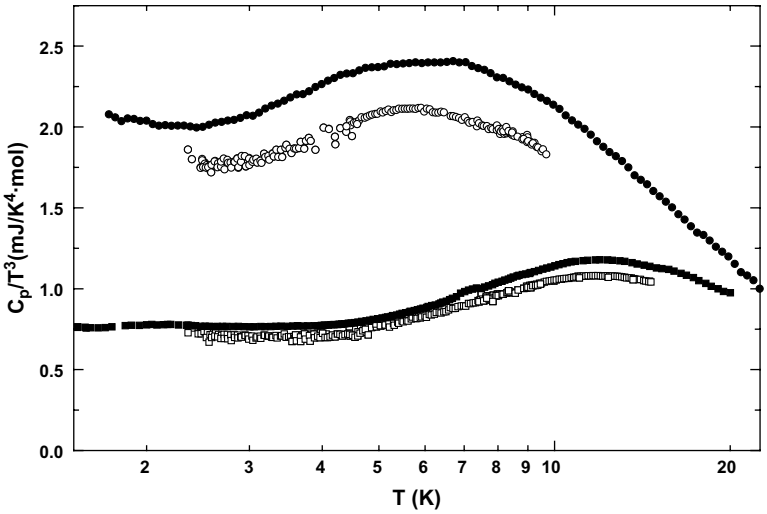

Fig. 6. Specific heat at low temperatures in a semilogarithmic C_p/T^3 vs T plot for glass (open circles) and crystal (open squares) phases of commercial (96% v/v pure, 3.4% H_2O) ethanol. For comparison, our previously published data [10,11] of the same phases but for pure ethanol are also shown with solid symbols.

4. Conclusions

We have presented a new experimental program for calorimetric experiments, allowing to tune adiabatic or continuous methods to monitor and characterize phase transitions at higher temperatures, and also two alternative thermal relaxation methods for low temperature specific heat measurements, depending on the value of the time constant which usually increases with temperature. The first experiments conducted with this program on different phases of ethanol in the range 2–20 K have been shown and briefly discussed, in comparison with previous data, when available. In particular, it has been found that γ and α crystalline phases have the same specific heat above 100 K, but seem to exhibit some difference at lower temperatures and hence in their elastic constants. We want to extend these more accurate specific heat measurements down to lower temperatures in order to reliably assess the linear and cubic coefficients of the different phases. Finally, we have also shown that less than 3.4% of water present in commercial (96% pure) ethanol is enough to eliminate the existence of the PC and ODC phases and hence to make this commercial ethanol a very good glass-former, related to a higher T_g and a lower T_m in comparison to pure ethanol. This 'commercial' ethanol glass also presents a lower specific heat than in pure ethanol.

Acknowledgments

We acknowledge the financial support by the Spanish Ministry of Education and Science within Project BFM-2003-04622.

References

[1] R.C. Zeller, R.O. Pohl, Phys. Rev. B 4 (1971) 2029.
[2] W.A. Phillips (Ed.), Amorphous Solids: Low Temperature Properties, Springer, Berlin, 1981.
[3] P.W. Anderson, Science 267 (1995) 1615.
[4] W.A. Phillips, J. Low Temp. Phys. 7 (1972) 351.
[5] P.W. Anderson, B.I. Halperin, C.M. Varma, Philos. Mag. 25 (1972) 1.
[6] D.A. Parshin, Phys. Rev. B 49 (1994) 9400.
[7] M.A. Ramos, U. Buchenau, in: P. Esquinazi (Ed.), Tunnelling Systems in Amorphous and Crystalline Solids, Springer, Berlin, 1998, p. 527 (Chapter 9).
[8] O. Haida, H. Suga, S. Seki, J. Chem. Thermodyn. 9 (1977) 1133.
[9] M.A. Ramos, S. Vieira, F.J. Bermejo, J. Dawidowski, H.E. Fischer, H. Schober, M.A. González, C.K. Loong, D.L. Price, Phys. Rev. Lett. 78 (1997) 82.
[10] C. Talón, M.A. Ramos, S. Vieira, Phys. Rev. B 66 (2002) 012201.
[11] M.A. Ramos, C. Talón, R.J. Jiménez-Riobóo, S. Vieira, J. Phys.: Condens. Mat. 15 (2003) S1007, and references therein.
[12] D.R. Lide (Ed.), Handbook of Chemistry and Physics, CRC Press, Boca Raton, FL, USA, 2005, p. 63 (Chapter 8).
[13] R. Bachmann, F.J. DiSalvo Jr., T.H. Geballe, R.L. Greene, R.E. Howard, C.N. King, H.C. Kirsch, K.N. Lee, R.E. Schwall, H.U. Thomas, R.B. Zubeck, Rev. Sci. Instrum. 43 (1972) 205.
[14] E. Gmelin, Thermochim. Acta 29 (1979) 1.
[15] M.A. Ramos, I.M. Shmyt'ko, E.A. Arnautova, R.J. Jiménez-Riobóo, V. Rodríguez-Mora, S. Vieira, M.J. Capitán, J. Non-Cryst. Solids 352 (2006) 4769.
[16] M.A. Ramos, V. Rodríguez-Mora, R.J. Jiménez-Riobóo, J. Phys.: Condens. Mat. 19 (2007) 205135, 10 p..